



## Microarticle

## A mini-phoswich scintillator as a possible stop detector for the NUMEN project

D. Carbone<sup>a</sup>, M. Cavallaro<sup>a</sup>, C. Agodi<sup>a</sup>, F. Cappuzzello<sup>a,b</sup>, L. Cosentino<sup>a</sup>, P. Finocchiaro<sup>a,\*</sup>, for the NUMEN collaboration<sup>a</sup> INFN Laboratori Nazionali del Sud, Catania, Italy<sup>b</sup> Dipartimento di Fisica e Astronomia, Università di Catania, Italy

## ARTICLE INFO

## Article history:

Received 5 September 2016

Received in revised form 7 October 2016

Accepted 10 October 2016

Available online 14 October 2016

## ABSTRACT

In the framework of the NUMEN project, aimed at the investigation of the nuclear matrix elements connected to the neutrinoless double beta decay by means of the Double Charge Exchange nuclear reactions (Cappuzzello et al., 2015), a high granularity stop detector for heavy ions is needed. It has to allow the identification of ions up to  $Z \approx 10$  while maintaining a total energy resolution around 2%. As the use of silicon detectors is not possible, due to their poor radiation hardness, scintillators are being investigated as possible candidates. In this paper we show a promising result obtained using a plastic + inorganic phoswich scintillator readout by means of a Silicon Photo Multiplier.

© 2016 The Authors. Published by Elsevier B.V. This is an open access article under the CC BY-NC-ND license (<http://creativecommons.org/licenses/by-nc-nd/4.0/>).

The stop detector foreseen for the NUMEN project [1] will be 100 cm wide and 20 cm high, placed at the exit of the gas chamber of the focal plane [2] of the MAGNEX magnetic spectrometer [3]. Its task is to support the identification of the impinging ions up to  $Z \approx 10$ , by means of the  $\Delta E$  vs  $E$  technique, and to reconstruct their residual energy with a precision of the order of a few percent [4]. A silicon telescope would be perfect for the task, as it is in the present focal plane detector. Unfortunately, due to the high counting rates expected, this solution is not enough radiation hard. Silicon Carbide semiconductor detectors are foreseen, as capable of fulfilling this task, but at the moment they are still under development [5].

The maximum expected counting rate on the stop detector is about 50 kHz/cm<sup>2</sup>, and the expected counting rate of the useful detected ions in the interest region defined by the MAGNEX setting is of the order of  $\leq 1$  Hz/cm<sup>2</sup> in the worst case. The single detector cell must be capable to handle such a rate and to withstand the corresponding radiation damage, also considering that the impinging particles will be heavy ions (as a reference one can consider <sup>16</sup>O at 20 MeV/amu). A reasonable geometry for the individual detector cell seems to be 1 cm × 1 cm, with the advantage of having all identical cells.

A possible candidate for the stop detector could have about 2500 cells, being each cell a 1 cm × 1 cm area phoswich made of a 200 μm thick fast plastic scintillator (Pilot-U) followed by a 5 mm thick CsI(Tl) inorganic scintillator. A thin aluminized mylar

reflector, 50 μm thick, covers the particle input face, whereas the four side faces are covered in white reflector. An energy loss calculation for the reference <sup>16</sup>O ion at 20 MeV/amu gives an energy deposition around 11 MeV in the aluminized mylar wrapping, 37 MeV in the  $\Delta E$  scintillator, with the residual 272 MeV deposited in the  $E$  scintillator. The light from such a detector can easily be collected by means of a SiPM, in particular the newly born 6 mm × 6 mm active area produced by SensL [6]. Fig. 1 shows the single components and a complete detector after its assemblage.

The radiation hardness of the proposed scintillators is not very high, but still much better than silicon, and basically resulting in a slight decrease of the light yield and of the light collection efficiency with the accumulated dose. A serious degradation is expected with a fluence above  $\approx 10^{13}$  particles/cm<sup>2</sup> (corresponding to about 1 ÷ 3 years of continuous experiment run as stop detector in the NUMEN conditions).

Two identical samples were assembled, and they were first tested with a <sup>22</sup>Na radioactive source. The source emits positrons, which immediately annihilate and produce 511 keV gamma rays, and also 1270 keV gamma rays. In Fig. 2 we show the persistence plot of the signals from the SiPM amplified by means of a voltage amplifier with gain 200 in order to be easily seen on the oscilloscope. The overall output signal duration is of the order of 1 μs, therefore indicating that the detector can safely sustain the expected maximum counting rate of 50 kHz.

In order to build the energy spectrum of the radioactive source the signal from the SiPM was directly fed into an ORTEC 855 spectroscopy amplifier with a 3 μs shaping time, whose output was

\* Corresponding author.

E-mail address: [finocchiaro@lns.infn.it](mailto:finocchiaro@lns.infn.it) (P. Finocchiaro).

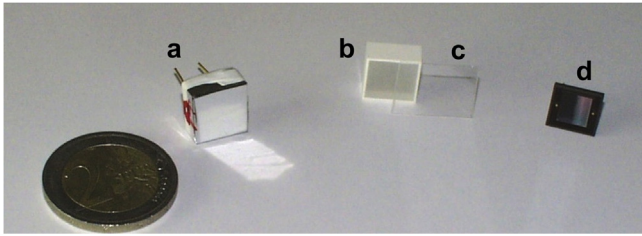


**Fig. 1.** (a) The phoswich detector cell wrapped in optical reflector, all parts optically coupled to each other. (b) The CsI(Tl) scintillator. (c) A piece of Plot-U fast plastic scintillator, before cutting it to the 1 cm × 1 cm size. (d) The 6 mm × 6 mm active area SiPM.

sent to a multichannel analyzer. Such a test only addressed the energy resolution of the CsI(Tl) scintillator section of the phoswich. The spectra taken with the two detectors, with a 14% FWHM resolution at 511 keV, are shown in Fig. 3. If we consider the reference case, with an energy deposition around 300 MeV and a reasonable factor 10 for the light quenching, we end up in a light signal around 30 MeV gamma equivalent, i.e. about 60 times the 511 keV gamma rays of the  $^{22}\text{Na}$  source [7]. Assuming a linear behaviour of the scintillator, the expected energy resolution should be of the order of  $14\%/\sqrt{60} \approx 2\%$  FWHM for the reference case.

A short beam test was performed at INFN-LNS with a 46 MeV  $^7\text{Li}$  beam, delivered by the Tandem accelerator, on a  $^7\text{LiF} + \text{C}$  target. The Phoswich “a” detector of Fig. 3 was placed 12 cm apart from the target at  $15^\circ$  (in this test and in the following one the “b” detector was placed at larger angles, thus collecting a smaller statistics; only data from “a” will be shown in the following). A BafPro filter & amplifier module [8], designed by INFN Milano, was used to replicate the detector signal in two copies, filtering out from one copy the fast light produced by the plastic scintillator, and amplifying both. By using the BafPro in this configuration we discovered that filtering out the fast component is by far more effective than selecting it. We built the scatter plot of Fig. 4 left, with the total light on the X-axis and the slow light (the only contribution from CsI(Tl)) on the Y-axis, and the righthand side being the same plot obtained with a 4x further amplification to explore a wider dynamic range. The Y values, as expected, are smaller, in proportion to their corresponding X values, for the ion species with higher atomic number Z. Therefore, the different species are separated on the plot, the higher the Z value the better the separation. This can

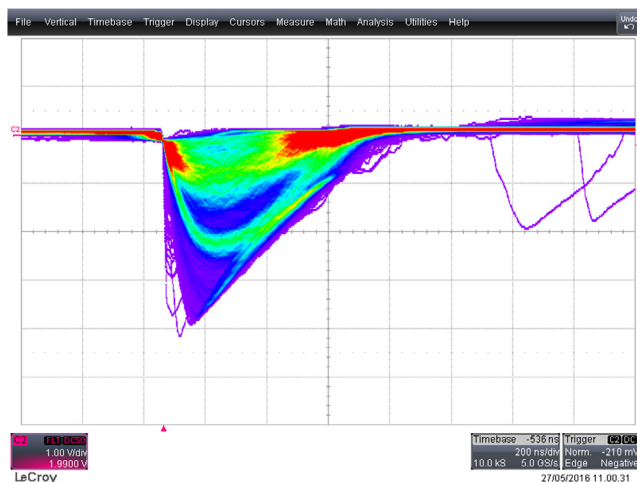


**Fig. 2.** Persistence plot of the output signals from the SiPM, amplified by means of a voltage amplifier with gain 200, produced when exposing the detector to a  $^{22}\text{Na}$  radioactive source. The 511 keV signal sticks out rather clearly.

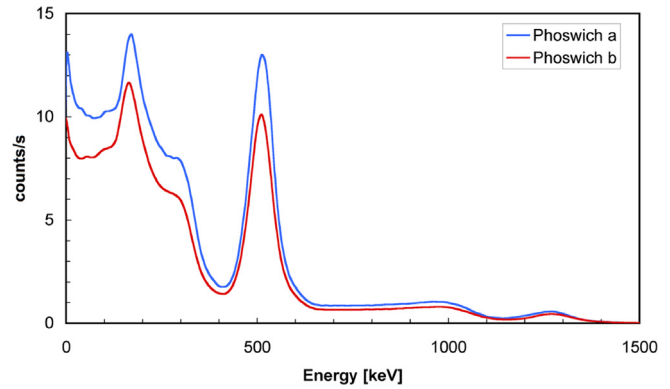


**Fig. 3.** Energy spectrum measured with the two phoswich detector cells. The radioactive source,  $^{22}\text{Na}$  emitting positrons (giving rise to 511 keV annihilation gamma rays) and 1270 keV gamma rays, was placed at slightly different distances from the two detectors. The resolution at 511 keV is 14% FWHM.

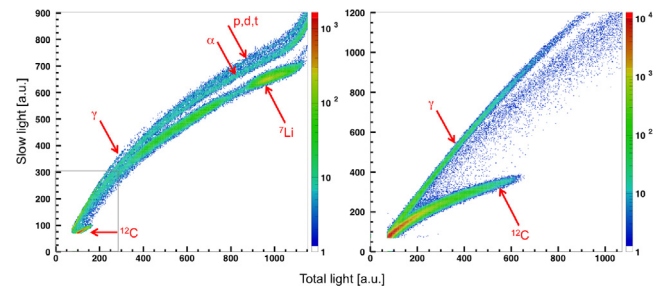


**Fig. 4.** Left: slow light versus total light for the 46 MeV  $^7\text{Li}$  on  $^7\text{LiF} + \text{C}$  test; five loci are visible corresponding to  $\gamma$ , (p,d,t),  $\alpha$ ,  $^7\text{Li}$ , and the low energy recoil  $^{12}\text{C}$ . Right: the same plot, obtained by applying a 4x amplification factor to both components, roughly corresponding to the rectangle in the lefthand figure.

be seen, for instance, in Fig. 4 where the separation between  $Z = 1$  and  $Z = 2$  is tiny whereas  $Z = 3$  is already well separated and  $Z = 6$  is very well separated.

By projecting the  $^7\text{Li}$  locus on the Y axis one obtains the plot of Fig. 5, where three main structures are visible, respectively due to the elastic scattering on the target elements  $^{19}\text{F}$ ,  $^{12}\text{C}$  and  $^7\text{Li}$ . In order to get a rough numerical estimate of the discrimination capability, we projected a vertical slice of Fig. 4 left, ten X-channels wide and centered on the  $^{19}\text{F}$  elastic peak, onto the Y axis. The resulting plot, shown in Fig. 6, has a peak and two small bumps corresponding to  $Z = 3$  ( $^7\text{Li}$ ),  $Z = 2$  ( $\alpha$ ) and  $Z = 1$  (p,d,t). The distance between the centroids of the  $^7\text{Li}$  peak and the  $\alpha$  bump corresponds to  $11.5 \sigma$  units ( $^7\text{Li}$ ) and to  $6.5 \sigma$  units ( $\alpha$ ). Moreover, such a distance is increasing with Z, thus hinting at an improving discrim-

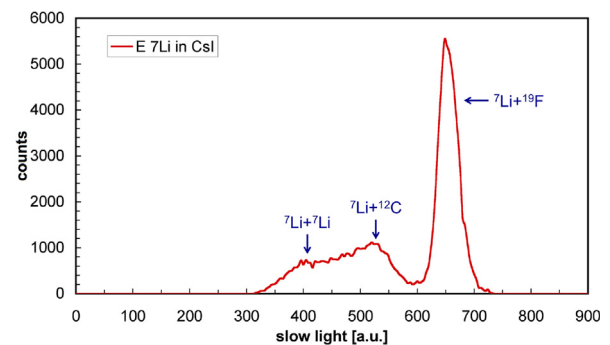


**Fig. 5.** Projection of the  $^7\text{Li}$  locus on the Y axis (slow light) for the 46 MeV  $^7\text{Li}$  on  $^7\text{LiF} + \text{C}$  test; three main structures are visible, respectively due to the elastic scattering on the target elements  $^{19}\text{F}$ ,  $^{12}\text{C}$  and  $^7\text{Li}$ .

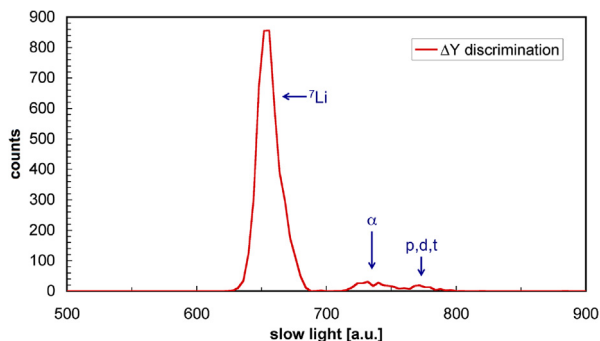


**Fig. 6.** Projection on the Y axis (slow light) of a vertical slice of Fig. 4, ten X-channels wide, centered on the  $^{19}\text{F}$  scattering peak. The peak and the two bumps correspond respectively to  $^7\text{Li}$ ,  $\alpha$  and (p,d,t), and prove that a good discrimination between different ion species is feasible.

ination for heavier particles. As the slow light is proportional to the residual energy in the CsI(Tl) scintillator, from both Fig. 5 and Fig. 6 we evaluated a FWHM energy resolution around 2.4% at the  $^7\text{Li} + ^{19}\text{F}$  elastic peak.

Another test was performed with a 320 MeV  $^{16}\text{O}$  beam on a  $^{27}\text{Al}$  target, by means of the LNS Cyclotron accelerator. The Phoswich “a” detector was placed at  $30^\circ$ . Fig. 7 shows the plots corresponding to those in Fig. 4, where the discrimination between  $\gamma$ , (p,d,t), and  $\alpha$  is even better due to their higher energy: indeed a hint of the deuteron locus is visible in Fig. 7 left. A cut and projection similar to the one done to produce Fig. 6 gives  $>11 \sigma$  units for the  $Z = 1$  to  $Z = 2$  separation, and inside  $Z = 1$  gives about  $4 \sigma$  units between protons and deuterons. The heaviest particle present on the plots in this case is  $^{16}\text{O}$ . Its residual energy resolution was evaluated in an X-slice fifty channels wide centered around  $X = 1725$  (from Fig. 7 right), by projecting such a slice on the Y axis where it roughly corresponds to an energy loss  $\approx 100$  MeV. The FWHM resolution resulted  $\approx 3.8\%$ , in line with the expectation for the reference case  $\left(3.8\% \cdot \sqrt{\frac{100\text{MeV}}{300\text{MeV}}} \approx 2.2\%\right)$ .

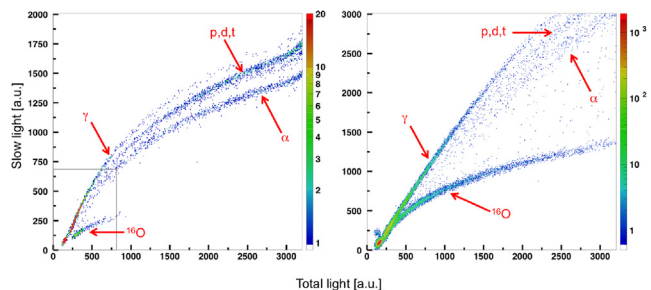


**Fig. 7.** Left: slow light versus total light for the 320 MeV  $^{16}\text{O}$  on  $^{27}\text{Al}$  test; several loci are visible corresponding to  $\gamma$ , (p,d,t),  $\alpha$ , and the quasi-elastic scattered  $^{16}\text{O}$ . Right: the same plot, obtained by applying a 4x amplification factor to both components, roughly corresponding to the rectangle in the lefthand figure.

In conclusion, the very compact, robust and inexpensive phoswich detector proposed as backup solution for NUMEN has shown quite interesting features, and promises to be a realistic candidate also for other applications needing the detection and identification of heavy ions.

### Acknowledgments

We thank D. Rizzo, S. Salamone, G. Passaro, B. Trovato, S. Di Modica, C. Marchetta, E. Costa, F. Tudisco, P. Reina for their invaluable support before and during the tests.

### References

- [1] Cappuzzello F et al. *Eur Phys J A* 2015;51:145.
- [2] Cavallaro M et al. *Eur Phys J A* 2012;48:59.
- [3] Cappuzzello F et al. *Eur Phys J A* 2016;52:167.
- [4] Cappuzzello F et al. *Nucl Instrum Meth A* 2010;621:419–23.
- [5] Muoio A. et al. *EPJ Web of Conferences*, vol. 117; 2016. p. 10006.
- [6] <<http://www.sensl.com/>>.
- [7] Sarantites DG et al. *Nucl Instrum Meth A* 2015;790:42–56.
- [8] Boiano C. et al. *IEEE Nuclear Science Symposium Conference Record N30-46*; 2008.